

Dynamic effects in electron-energy-loss processes in barium, lanthanum, and cerium

J. Kanski

Department of Physics, Chalmers University of Technology, S-412 96 Gothenburg, Sweden

G. Wendin

Department of Theoretical Physics, Chalmers University of Technology, S-412 96 Gothenburg, Sweden

(Received 16 March 1981)

Electron-energy-loss spectra of barium, lanthanum, and cerium in the regions of $3d$ -level excitations have been found to show doublet structures associated with each spin-orbit component. The relative intensities of the structures vary systematically with excitation energy. One of the doublet components can in each case be associated with a $3d \rightarrow 4f$ excitation. For the explanation of the second component we propose a process which involves decay of an intermediate screened $3d^9 4f^2$ state.

Recent detailed investigations of x-ray emission (XES) from lanthanum¹ and cerium² have revealed that apart from the "normal" characteristic lines (including so-called resonance emission), there appear additional lines when the initial core-hole states are excited with electrons whose energies just exceed the core-hole excitation thresholds. These anomalous lines, which appear as satellites 2–3 eV below the $M_{\alpha,\beta}$ bands, were first associated with resonant bremsstrahlung.^{1,2} In a previous paper³ we pointed out that such an interpretation is inconsistent with the fact that these lines are present with appreciable intensity also for excitation energies well off resonance energies. We also presented evidence in the form of electron-energy-loss spectra (EELS) that in the case of lanthanum the mechanism behind these emission lines is of the characteristic kind; i.e., the lines represent electronic transitions between discrete states of the actual system. In the process of identification of the anomalous lines in threshold excited XES, it is important to establish that the close correspondence between EELS and XES found for lanthanum is not accidental. It is also essential to estimate the role of the $4f$ orbitals in the production of these lines. For this purpose we compare in this paper EELS data of barium, lanthanum, and cerium. Although these elements are neighbors in the periodic table, their electron structures differ qualitatively. The transition from barium to lanthanum leads to localization of the $4f$ orbitals, but they remain unoccupied. With a vacancy in the $3d$ shell we know that the $4f$ state becomes populated in lanthanum⁴ (the energy of the $3d^9 4f^1$ configuration is clearly lower than that of $3d^9 4f^0$). Such population does not occur in barium, but $4f$ orbitals are likely to be localized as in the ground state of lanthanum. Cerium

differs from the two preceding elements in that it contains a $4f$ electron in the ground state. This leads, for instance, to quite pronounced multiplet splitting in x-ray-absorption spectra⁵ (XAS).

The energy-loss data reported here were obtained with a conventional single-pass cylindrical-mirror analyzer (CMA) with an integral electron gun. The spectra were recorded in a constant-final-energy mode, which means that the pass energy of the CMA was kept at a constant, arbitrarily chosen value, while the energy of the primary electron beam was scanned continuously. There are several advantages with this mode of operation. First, the energy calibration is obtained simply by measuring the potential applied to the electron source. Energy scale distortions which may plague CMA optics with imperfect focusing and sample location are thus eliminated. Second, since the pass energy is kept constant, the energy resolution is constant throughout a spectrum. Third, the appearing structures can immediately be classified as characteristic energy losses, with no risk of confusion with Auger structures. The energy of the primary electrons as they hit the sample is given by the potential difference between the electron source and the sample. With a given analyzer pass energy eV_p and a sample potential V_s , the energy of electrons which will be transmitted through the analyzer is $e(V_s + V_p)$ when they are at the sample. This energy will be referred to as the final energy.

To obtain good energy resolution one should operate at a low pass energy. However, with decreasing pass energy the analyzer transmission function also decreases. Another limiting factor is an increasing intensity of secondary electrons towards low energies. As a compromise to these considerations our data were recorded at pass energies 100–200 eV.

A very interesting observation was that the choice of final energy affected the relative intensities of the energy-loss structures. We have reported this effect previously for $3d$ excitations in lanthanum,³ and will examine it below in the case of barium and cerium.

Figures 1, 2, and 3 show the energy loss spectra of barium, lanthanum, and cerium, obtained at 100-, 150-, 300-, and 600-eV final energies. The similarities between the three sets of data are evident. In all cases the energy losses are divided into two groups, corresponding to excitations of the $3d_{5/2}$ and $3d_{3/2}$ levels. Each group contains in turn two peaks, which appear somewhat more distinct for the $3d_{5/2}$ levels. There is a clear systematic redistribution of the relative intensities of these peaks with changing final energy: at low final energies the low-energy components in each doublet tend to dominate. With increasing final energies the high-energy components gain in relative intensities. We note further that the relative intensities of the low-energy components are smaller throughout in the $3d_{3/2}$ than in the $3d_{5/2}$ doublets. The energy range over which the intensity redistribution takes place increases when going from barium to cerium.

In Fig. 4 we compare our EELS data with the corresponding XAS and XES results from the literature^{1,2,5} for lanthanum and cerium. Barium is not included due to lack of data in the literature. Before

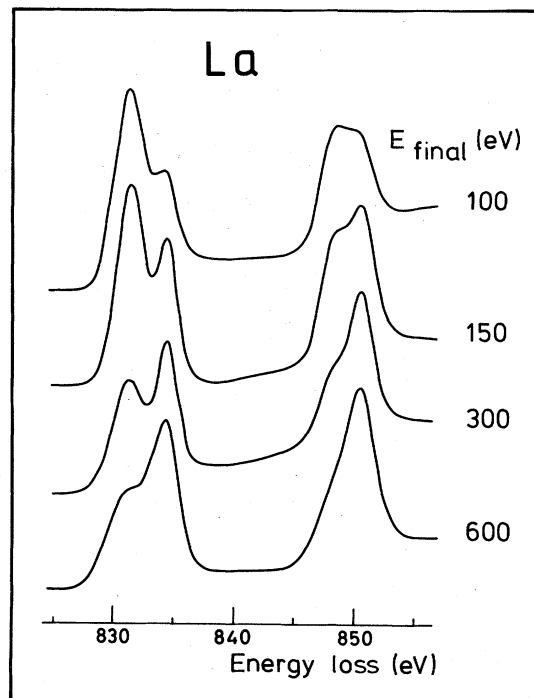


FIG. 2. Electron-energy-loss spectra of lanthanum.

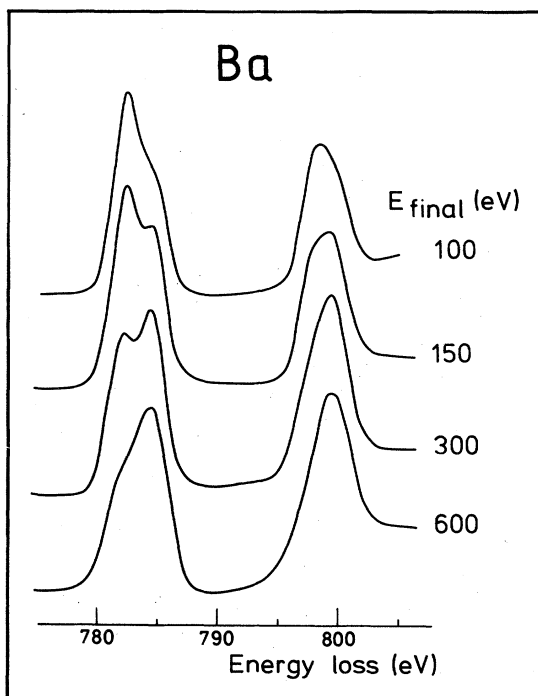


FIG. 1. Electron-energy-loss spectra of barium covering the region of $3d$ level excitations.

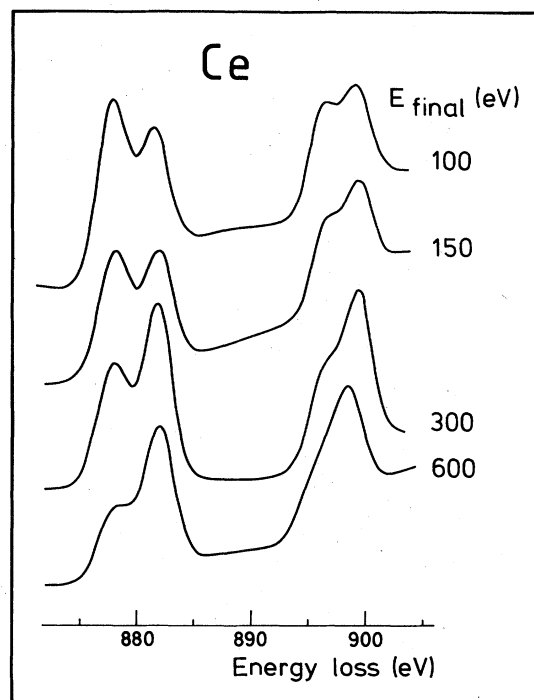


FIG. 3. Electron-energy-loss spectra of cerium.

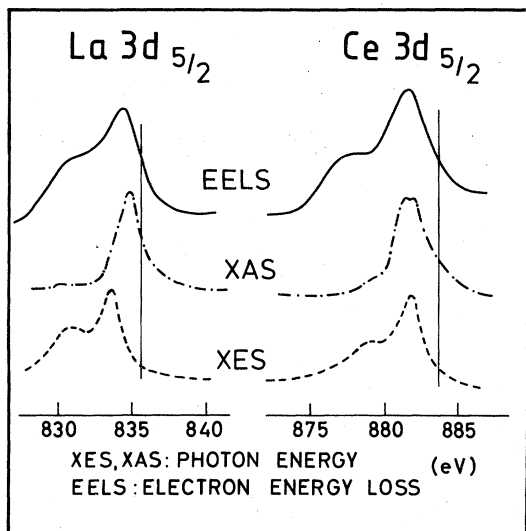


FIG. 4. Comparison of electron-energy-loss x-ray absorption (Ref. 5) and x-ray emission (Refs. 1 and 2) spectra for lanthanum and cerium. The vertical lines indicate the $3d_{5/2}$ level binding energies as given by XPS (Ref. 7).

further discussion it should be pointed out that none of the spectra in Fig. 4 has been shifted in energy from the position given in the original work. Considering all difficulties associated with absolute energy calibration of x-ray spectrometers, there is without doubt room for small energy adjustments. We know for instance that the main lines in XES and XAS spectra of lanthanum reflect the same transitions and do in fact coincide when recorded with the same instrument.⁶ However, since the spectra of cerium are somewhat complex, we have chosen not to make any energy alignments here.

Again we recognize similarities between the sets of lanthanum and cerium data. First of all we note that all spectral features appear *below* the $3d_{5/2}$ XPS binding energies,⁷ which represent final states without $4f$ screening (i.e., $3d^9 4f^0$ and $3d^9 4f^1$ configurations in lanthanum and cerium, respectively). Next, we see that both XES spectra, which were excited with electrons of energies about 50 eV in excess of ionization thresholds, contain one major peak with a shoulder-like peak at the low-energy side. Within the experimental accuracy the main XES peaks coincide in energy with the main absorption lines in XAS and also with the high-energy components in the EELS doublets. In the case of lanthanum the shoulder in XES does clearly not have any counterpart in XAS. Any correspondence with the faint peak at 830 eV is excluded mainly because of different energy separation from the main line (4.9 eV compared to 2.8 eV in XES), and also because of the very different relative

intensity. For cerium the situation is less clear due to multiplet splitting. In the absorption spectrum one can distinguish three lines associated with excitation of the $3d_{5/2}$ spin-orbit level. One of these lines appears as a shoulder at the low-energy side of a doublet complex. Since the absorption spectrum falls below the $3d$ binding energy as noted above, one should in principle be able to observe the same lines in XES.⁸ In fact, when excited with high-energy electrons, the $3d_{5/2}$ emission spectrum does exhibit all the features of the absorption spectrum.⁹ Therefore, it is less obvious in the case of cerium than for lanthanum that there appears a completely new emission line in threshold excited XES. However, considering the similarities in the development of emission spectra of lanthanum and cerium around threshold excitations, there is good reason to believe that the low-energy component in XES of cerium in Fig. 4 reflects a process absent in XAS. Its shape and exact energy position may be influenced by an underlying structure corresponding to the shoulder in XAS.

One very important observation that can be made in Fig. 4, and which has been pointed out previously,³ is the close similarity between the EELS and XES results for lanthanum. In the case of cerium the correspondence between EELS and XES structures is not as obvious as the separation between the two peaks in EELS is about 0.7 eV larger than in XES. As pointed out above, the apparent energy separation between the two peaks in XES may be influenced by an underlying structure corresponding to the shoulder in XAS. Thus, considering the similar energy dependence of the low-energy EELS and XES structures (in both experiments they appear with maximum relative intensity for excitations close to threshold, and vanish at high excitation energies), we believe they originate from basically the same process.

Structures in EELS correspond of course to characteristic excitation processes. To identify energy-loss spectra it is therefore natural to make comparison with x-ray absorption data. From Fig. 4 it follows that the high-energy components in the EELS doublets can be identified with x-ray absorption lines in lanthanum and cerium. Photoelectron yield measurements on barium¹⁰ show that also in this case the high-energy EELS components (Fig. 1) can be associated with photoabsorption lines. The low-energy components in the EELS doublets are, however, absent in all x-ray absorption spectra.

There are several mechanisms which in principle can give rise to differences between EELS and XAS data and could be considered as candidates for the origin of the low-energy EELS components.

(1) The two methods of course test quite different sample regions. EELS is extremely surface sensitive, while XAS in contrast probes the bulk. The low-energy components in EELS could therefore originate from excitations at the surface.

(2) An obvious distinction between EELS and XAS is that in the latter case only those excitations which obey the dipole selection rule can be observed. In EELS the excitations are promoted through Coulomb interaction between core and projectile electrons. The energy losses are observed in the beams of back scattered electrons in a wide space angle. Therefore no strict selection rules with respect to angular momentum transfer apply in this case. We note also that similar divergences between EELS and photoabsorption spectra have been observed in, e.g., the excitation spectra of helium, in which case the differences were explained successfully in terms of different excitation matrix elements.^{11,12}

(3) An effect which could in principle give doublet structures in EELS is varying degree of final-state screening. In the case of $3d$ level excitations in rare-earth metals the $3d$ hole can be screened very efficiently by an additional $4f$ electron. Through population of a $4f$ orbital the energy of the system can be lowered. Detailed examinations of x-ray photoelectron spectra (XPS) of the light rare-earth metals⁷ have shown that the most intense $3d$ emission lines have satellites on their high kinetic energy sides. The satellites correspond to well screened (relaxed) final states, including "shake-down" populated $4f$ orbitals. In lanthanum for instance the equivalent binding energy corresponding to the main $3d_{5/2}$ line is 835.8 eV, while the satellite is centered around 832.5 eV. This energy is clearly lower than the $3d^9 4f^1$ energy (~ 834.0 eV) observed in XAS. The difference could be taken as an indication of further relaxation in the final state corresponding to the XPS satellite. Within this framework the two energy-loss structures in each doublet could correspond to well and poorly screened $3d^9 4f^1$ states, respectively.

All these explanations are, however, met by contradicting experimental observations. If the doublet structures in EELS were due to excitations at and beneath the surface layer, one would definitely expect the spectra to be sensitive to the surface conditions. Experimentally we have found (not shown here) that EELS results on clean metal surfaces (as judged by Auger electron spectroscopy) are practically identical with those obtained on purposely oxidized samples. Next, we note that the similarities between the EELS data observed in Figs. 1–3 suggest that the origin of the doublet structures is unlikely to be multiplet splitting of one configuration (e.g., $3d^9 4f^{n+1}$), since the multiplet structures of barium and lanthanum are essentially different from that of cerium.⁵ Also, if our identification of the low-energy components in EELS and XES is correct, the absence of these structures in XAS can clearly not be due to vanishing dipole matrix elements for the corresponding transitions. There is another, independent piece of experimental indication that the origin of the low-energy components in EELS is more complex than

suggested by any of the above-mentioned mechanisms. According to Figs. 1–3 the relative intensities of these components increase with decreasing primary electron energy. Despite this, no $3d$ excitations are observed in electron excited APS data at the energies of the low-energy components.³ In contrast, excitation thresholds are observed at primary electron energies equal to those of the high-energy EELS components.

From the fact that the low-energy lines are not observed in XAS and APS, we draw the important conclusion that the *lower energy state*, which is involved in the electronic transitions observed via these lines, is not the ground state of the system, but an *excited state*. Threshold excited XES data clearly show^{13,14} that this emission appears strongly enhanced under conditions when it coincides in energy with the $4f$ bremsstrahlung emission. This strongly suggests that the excited lower energy state in XES and EELS is $\{M\}4f^1$, i.e., the same as the final state in $4f$ bremsstrahlung emission (M represents here the ground-state configuration of barium, lanthanum, and cerium, respectively). It appears quite straightforward to ascribe the low-energy lines in XES and EELS to transitions of the type



($n=0$ for barium and lanthanum and $n=1$ for cerium).

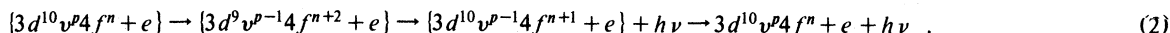
Of course, the question now arises how these transitions are involved in the XES and EELS processes. In XES they may be present as a consequence of shake-up excitations of $3d^9 4f^{n+2}$ states which decay to $3d^{10} 4f^{n+1}$. This can occur over a wide excitation energy range. It is more difficult to see how these transitions can be excited in EELS. Since the $3d^{10} 4f^{n+1}$ state is in all cases an excited state, the excitations reflected by the energy-loss structures could in principle be the results of two processes, namely, the primary excitation of $3d^{10} 4f^{n+1}$ followed by an independent second excitation to $3d^9 4f^{n+2}$. Such two step excitation would require either very long-lived intermediate $3d^{10} 4f^{n+1}$ states, or very high primary current densities to maintain a population of the $3d^{10} 4f^{n+1}$ states. None of these requirements is fulfilled here. The lifetime width of the $3d^{10} 4f^{n+1}$ state is ~ 1 eV for the three elements corresponding to lifetimes of $\sim 10^{-15}$ s. With a primary current density of ~ 10 mA/cm² as in the present experiments, a target section of a typical core level cross section dimension ($\sigma = 10^{-18}$ cm²) is hit by less than 1 projectile electron per second. Therefore, double excitations by independent events are negligible.

Since the XES spectra indicate radiative decays of shake-up states, one would expect to observe structures in EELS at energies corresponding to excitations of these states, provided they are produced in

single excitation processes. In the case of lanthanum the threshold energy for $3d^9 4f^2$ excitation is 836.8 eV as determined by APS. Detailed examinations of EELS spectra around this energy do not, however, reveal any structure corresponding to such excitations. From this we conclude that the excitation and

decay processes are unseparable and furthermore that the interaction between projectile electrons and scattering center does not cease until the scatterers have returned to their ground state.

The XES and EELS processes enter thus as components in one chain of transitions



The brackets indicate complexes of interacting particles and v^p are valence-band electrons. In Fig. 5 we show some fundamental excitation and emission processes that we think might account for the observed EELS and XES spectra.¹⁵ Figure 5(a) represents near threshold excitation where the incident electron creates a negative-ion resonance in the form of a localized $3d^9 4f^2$ level. The radiative decay of this level leaves a localized $4f$ electron and a photon with 831-eV energy. The decay of the $3d^9 4f$ electron-hole pair thus takes place in the presence of a localized $4f$ electron, which can adjust to the new potential after the decay has taken place. Excitation and emission become coherent and inseparable.

Another way to look upon the process in Fig. 5(a) is in terms of resonant bremsstrahlung, as discussed by Wendin and Nuroh.¹⁶ Figure 5(b) describes excitation of a $3d^9 4f$ electron-hole pair in the case where the projectile goes into a delocalized final state. In this case the projectile cannot perturb the decay process: excitation and decay become independent processes and emission occurs at ~ 834 eV. This would, e.g., be the case if the projectile is very fast, in which case the final-state energy will be high, and the projectile will leave the interaction region very

rapidly. In an intermediate situation where the projectile leaves the interaction region on a time scale comparable to the decay time, one can expect to see two emission lines, at ~ 831 and ~ 834 eV and with intensity being transferred from the 831-eV line to 834-eV line with increasing energy of the final-state electron. This is precisely the picture given by the experimental results in Fig. 1 and suggests that we are dealing with post-collision interaction^{17,18} (PCI) and incomplete relaxation¹⁹ types of processes. One remarkable thing is, however, that experiments show that the intensity transfer occurs very slowly over a large range (~ 500 eV) of final-state energies. We have no quantitative explanation for how this comes about. Qualitatively, however, we think this can be explained in terms of transient response and dynamical screening in the final state. In Fig. 5(a), the incident electron has high-energy E (~ 800 eV) and will be fairly poorly screened. After sudden creation of a localized $3d^9 4f^2$ excitation, this state has to be screened by surrounding the excitation with a neutralizing correlation hole, i.e., by displacing one unit of electronic charge out of the unit cell.

Figure 5(c) shows one contribution to this screening process, which obviously leads to a coupling between the processes in Figs. 5(a) and 5(b) and thus provides one mechanism for intensity transfer between the 831- and 834-eV lines. This process has the desired property that it always leads to a screened $3d^9 4f^2$ intermediate level, with the excess energy carried away by a continuum electron. Figure 5(d) shows our conception of the dynamically screened intermediate level in real space. At threshold energy the excitation will be introduced adiabatically and no excess energy has to be carried away. As the final-state energy is raised, the screening process becomes transient and we get a picture of a screened intermediate excitation with a wave propagating away with the excess energy. Decay then takes place in the same local environment as in the threshold case, yielding an x-ray emission line at 831 eV. Finally, the change in potential due to the emission process can scatter the $4f$ electron into the correlation hole and transfer energy and angular momentum to the receding continuum electron, scattering it into $\epsilon'f$. The $\epsilon'g$ wave has large overlap with $4f$ over an energy range of several hundred eV,^{15,16} and that is why

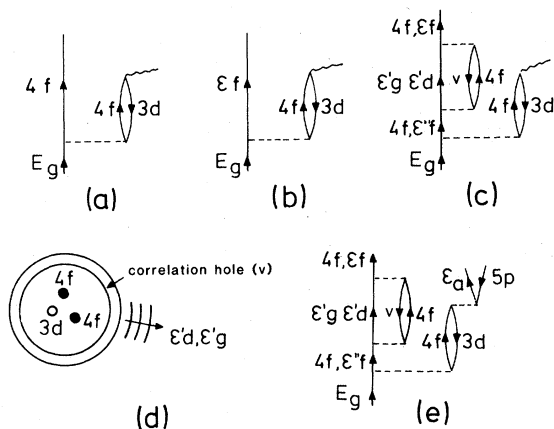


FIG. 5. Diagrammatic and real-space pictures of excitation and emission processes (see text). (a)–(c) Describe x-ray emission while (e) describes autoionization. (d) Illustrates our conception of the screened quasilocated $3d^9 4f^2$ level.

we think the proposed process might play a part in feeding intensity into the 831-eV line. We think that it is essential that there is high probability for the pickup process to occur, because only then will an energy loss of 831 eV be detected in EELS. In the opposite case, the loss would occur at 837 eV, which is not supported by experiment.

As the final-state energy is raised, the screening process will be less efficient and the probability for leaving the system in the configuration shown in Fig. 5(b) will be less and less probable. The process in Fig. 5(d) will then take over and the 834-eV line will grow to be the dominant one both in EELS and XES.

Let us finally remark that the time scale of decay is set by x-ray emission in combination with autoionization and Auger processes. Consequently, part of the EELS intensity should be associated with scattering together with nonradiative decay, as shown by the example in Fig. 5(e) (cf. Ref. 18). It follows then that various autoionization lines should exhibit double structures and intensity variations similar to those seen in EELS.

In conclusion, the data presented here show that anomalous structures in EELS similar to those found previously for lanthanum are also present in the spectra of barium and cerium. Both for lanthanum and

cerium these structures appear to correspond to emission lines in XES. No XES data are available as yet for metallic barium. On the basis of our EELS results and on the general similarities between the spectroscopic properties of barium and the light rare-earth metals, we expect the threshold excited $3d_{5/2}$ emission spectrum of barium to show a strong line at ~ 782 eV, which decreases in intensity with increasing excitation energy.

Several different possible explanations for the observed structures have been considered and some have been rejected due to inconsistency with the combined experimental information. Our final tentative interpretation suggests that the anomalous structures in EELS and XES represent transitions between two excited states of the system.

It has also come to our attention that observations similar to those reported here have been indicated previously in an abstract of a conference report.²⁰

ACKNOWLEDGMENTS

The authors acknowledge useful discussions with Professor P. O. Nilsson. This work was supported by grants from the Swedish Natural Research Council.

-
- ¹R. J. Liefeld, A. F. Burr, and M. B. Chamberlain, *Phys. Rev. A* **9**, 316 (1974).
- ²M. B. Chamberlain, A. F. Burr, and R. J. Liefeld, *Phys. Rev. A* **9**, 663 (1974).
- ³J. Kanski and P. O. Nilsson, *Phys. Rev. Lett.* **43**, 1185 (1979).
- ⁴J. Kanski, P. O. Nilsson, and I. Curelaru, *J. Phys. F* **6**, 1073 (1976).
- ⁵C. Bonnelle, R. C. Karnatak, and J. Sugar, *Phys. Rev. A* **9**, 1920 (1974).
- ⁶J. M. Mariot and R. C. Karnatak, *J. Phys. F* **4**, L223 (1974).
- ⁷G. Crecelius, G. K. Wertheim, and D. N. E. Buchanan, *Phys. Rev. B* **18**, 6519 (1978).
- ⁸J. Kanski (unpublished).
- ⁹R. C. Karnatak, Ph. D. thesis (University of Paris, 1971) (unpublished).
- ¹⁰J. Kanski and P. O. Nilsson, *Phys. Scr.* **12**, 103 (1975).
- ¹¹J. A. Simpson, G. E. Chamberlain, and S. R. Mielczarek, *Phys. Rev.* **139**, A1039 (1965).
- ¹²R. P. Madden and K. Codling, *Phys. Rev. Lett.* **10**, 516 (1963).
- ¹³P. Motais, E. Belin, and C. Bonnelle, in *Proceedings of the International Conference on X-ray Processes and Inner-Shell Ionization*, Stirling, 1980 (unpublished).
- ¹⁴F. Riehle, *Jpn. J. Appl. Phys. Suppl.* **2**, **17**, 314 (1978).
- ¹⁵G. Wendin and K. Nuroh (unpublished).
- ¹⁶G. Wendin and K. Nuroh, *Phys. Rev. Lett.* **39**, 48 (1977); K. Nuroh, *Phys. Scr.* **21**, 519 (1980); K. Nuroh and G. Wendin (unpublished).
- ¹⁷G. Wendin, Daresbury Laboratory Report No. DL/SCI/RII (unpublished), pp. 1–21.
- ¹⁸M. Ya. Amusia, M. Yu. Kuchiev, and S. A. Sheinerman, in *Coherence and Correlation in Atomic Collisions*, edited by H. Kleinpoppen and J. F. Williams (Plenum, New York, 1980), p. 297–313.
- ¹⁹For discussion and further references, see L. Hedin, *J. Phys. (Paris)* **39**, C4-103 (1978); J. C. Fuggle, R. Lässer, O. Gunnarsson, and K. Schönhammer, *Phys. Rev. Lett.* **44**, 1090 (1980); O. Gunnarsson and K. Schönhammer, *Phys. Rev. B* **22**, 3710 (1980).
- ²⁰I. B. Borovskii and E. J. Komarov, *Jpn. J. Appl. Phys. Suppl.* **2**, **17**, 237 (1978).